



Published in final edited form as:

Biochem Pharmacol. 2015 December 15; 98(4): 602–613. doi:10.1016/j.bcp.2015.10.015.

Combination therapy with bioengineered miR-34a prodrug and doxorubicin synergistically suppresses osteosarcoma growth

Yong Zhao^{1,2}, Mei-Juan Tu², Yi-Feng Yu¹, Wei-Peng Wang², Qiu-Xia Chen², Jing-Xin Qiu³, Ai-Xi Yu¹, and Ai-Ming Yu²

¹Department of Orthopedics, Zhongnan Hospital of Wuhan University, Wuhan, Hubei 430070, China

²Department of Biochemistry & Molecular Medicine, UC Davis School of Medicine, Sacramento, CA 95817, USA

³Department of Pathology, Roswell Park Cancer Institute, Buffalo, NY 14263, USA

Abstract

Osteosarcoma (OS) is the most common form of primary malignant bone tumor and prevalent among children and young adults. Recently we have established a novel approach to bioengineering large quantity of microRNA-34a (miR-34a) prodrug for miRNA replacement therapy. This study is to evaluate combination treatment with miR-34a prodrug and doxorubicin, which may synergistically suppress human OS cell growth via RNA interference and DNA intercalation. Synergistic effects were indeed obvious between miR-34a prodrug and doxorubicin for the suppression of OS cell proliferation, as defined by Chou-Talalay method. The strongest antiproliferative synergism was achieved when both agents were administered simultaneously to the cells at early stage, which was associated with much greater degrees of late apoptosis, necrosis, and G2 cell cycle arrest. Alteration of OS cellular processes and invasion capacity was linked to the reduction of protein levels of miR-34a targeted (proto-)oncogenes including SIRT1, c-MET, and CDK6. Moreover, orthotopic OS xenograft tumor growth was repressed to a significantly greater degree in mouse models when miR-34a prodrug and doxorubicin were co-administered intravenously. In addition, multiple doses of miR-34a prodrug and doxorubicin had no or minimal effects on mouse blood chemistry profiles. The results demonstrate that combination of doxorubicin chemotherapy and miR-34a replacement therapy produces synergistic antiproliferative effects and it is more effective than monotherapy in suppressing OS xenograft

Address correspondence to: Prof. Dr. Ai-Xi Yu, Department of Orthopedics, Zhongnan Hospital of Wuhan University, Wuhan, Hubei 430070, China; yuaixi@whu.edu.cn; or Prof. Ai-Ming Yu, Department of Biochemistry & Molecular Medicine, UC Davis School of Medicine, Sacramento, CA 95817, USA; aimyu@ucdavis.edu.

Publisher's Disclaimer: This is a PDF file of an unedited manuscript that has been accepted for publication. As a service to our customers we are providing this early version of the manuscript. The manuscript will undergo copyediting, typesetting, and review of the resulting proof before it is published in its final citable form. Please note that during the production process errors may be discovered which could affect the content, and all legal disclaimers that apply to the journal pertain.

Authors' Contributions: All authors participated in research design, performed data analyses, and contributed to writing, revising, and final approval of the manuscript. Y Z, M-J T, W-P W, Q-X C, and J-X Q conducted the experiments. A-M Y and A-X Y contributed to new reagents and analytical tools.

Conflict of Interests: The authors declare that they have no conflict of interests.

tumor growth. These findings support the development of mechanism-based combination therapy to combat OS and bioengineered miR-34a prodrug represents a new natural miRNA agent.

Keywords

Osteosarcoma; miR-34a; doxorubicin; chemotherapy; orthotopic tumor

1. Introduction

Osteosarcoma (OS) is the most common form of primary malignant bone tumor, which is locally destructive by producing malignant osteoid or immature bone. Accounting for approximately 60% of malignant bone tumors, OS is the most prevalent among children and young adults [1-3]. Although some options including complete resection of the tumor tissues and chemotherapy with high-dose methotrexate, doxorubicin, and cisplatin (sometimes with ifosfamide) are available for the treatment of OS, about 30% of OS patients would not be able to survive over five years. Because OS has a high potential for pulmonary metastasis [4-6], most OS patients may eventually die of pulmonary metastases. Therefore, there is a clear need for the development of new and more effective therapeutics to combat malignant OS [7, 8].

MicroRNAs (miRNAs or miRs) are a large family of small noncoding RNAs (ncRNAs) that are derived from human genome and responsible for posttranscriptional regulation of numerous target genes underlying various cellular processes including cancer cell proliferation and tumor progression [9-11]. With an improved understanding of miRNA cancer biology, there has been a growing interest in developing miRNA-based therapies [12-14]. Of particular note, some tumor suppressing miRNAs, such as miR-34a, depleted in cancerous tissues may be reintroduced into cancer cells to control cancer cell growth and tumor progression [15-17]. Indeed miR-34a is a direct target of p53 and it exhibits strong antiproliferative activity against a variety of cancer cells through targeting of many (proto-)oncogenes, such as NAD-dependent deacetylase sirtuin-1 (SIRT1), cyclin-dependent kinase 6 (CDK6), hepatocyte growth factor receptor c-MET, and cell surface glycoprotein CD44, which regulate apoptosis, cell cycle, invasion, and other cellular processes [18-21]. Co-administration of miR-34a also increases the sensitivity of human carcinoma cells to chemotherapeutics, e.g., bladder cancer cells to cisplatin [22], and triple negative breast cancer cells to doxorubicin [23]. Additionally, a liposome-formulated miR-34a, namely “MRX34”, has entered Phase I clinical trials for the treatment of unresectable primary liver cancer [24].

Recent studies have also revealed that miR-34a is significantly downregulated in human OS tissues, and a lower miR-34a level may forecast a notably poor disease-free survival rate in OS patients [25-27]. Furthermore, restoration of miR-34a function in OS cells using synthetic miR-34a mimics reduces cell proliferation *in vitro*, and forced expression of miR-34a in OS cells not only inhibits cell proliferation *in vitro* but also represses tumorigenesis *in vivo* [26-29]. Nevertheless, there is no report thus far on the utility of

systemic administration of a miR-34a agent or combination of miR-34a and chemotherapeutic drug for the treatment of OS in a whole body system.

Aiming to develop miRNA-based therapy, we have developed a novel approach to bioengineering large quantities of miR-34a prodrug [30, 31]. These genetically engineered miRNA agents are distinguished from synthetic miRNA agents (e.g., miRNA mimics or pre-miRNAs) for being produced and folded within live cells, which should better capture the function and safety properties of natural RNAs [30, 32, 33]. Indeed biological miR-34a prodrug is selectively processed to mature miR-34a in human lung carcinoma cells, and consequently reduces cancer cell proliferation *in vitro* and inhibits xenograft tumor growth *in vivo* [30]. However, bioengineered miR-34a prodrug often exerts a partial inhibition against human carcinoma cells, similar as synthetic miR-34a agents. On the other hand, high-dose doxorubicin chemotherapy may completely inhibit cancer cell growth but also produce toxic effects [34]. Therefore, in the present study, we aimed to evaluate the utility of combination therapy with bioengineered miR-34a prodrug and doxorubicin for the treatment of OS. Acting through RNA interference and DNA intercalation, miR-34a and doxorubicin combination treatment could produce synergistic effects in the control of cancer cell growth (Figure 1), and thus much lower and safe doses may be used to achieve the same efficacy and minimize or avoid toxicity [35-37]. We then delineated the synergism and mechanistic actions of combination therapy in the inhibition of OS cell proliferation in human OS cells *in vitro*, and defined the effectiveness and safety profiles of miR-34a prodrug and doxorubicin co-administered intravenously in an orthotopic OS xenograft tumor mouse models *in vivo*.

2. Materials and Methods

2.1. Materials

Doxorubicin hydrochloride salt (> 98%) was purchased from Sigma-Aldrich (St. Louis, MO, USA). 3-(4,5-Dimethylthiazol-2-yl)-2,5-diphenyltetrazolium bromide (MTT), Trizol reagent, BCA Protein Assay Kit, and Lipofectamine 2000 were purchased from Thermo Fisher Scientific Inc. (Waltham, MA, USA). RPMI 1640 medium, trypsin and phosphate-buffered saline were bought from GE Healthcare Bio-Sciences (Pittsburgh, PA, USA). Fetal bovine serum was purchased from GBICO BRL (Rockville, MD, USA). RIPA lysis buffer was bought from Rockland Immunochemicals (Limerick, PA, USA), and protease inhibitor cocktail was from Roche Diagnostics (Mannheim, Germany). ECL substrate and PVDF membrane were purchased from Bio-Rad (Hercules, CA, USA). Annexin V-FITC conjugate and propidium iodide solution was purchased from Trevigen Inc. (Gaithersburg, MD, USA), and PI/RNase Staining Buffer was from BD Biosciences (San Jose, CA, USA). All other chemicals and organic solvents of analytical grade were purchased from Sigma-Aldrich or Thermo Fisher Scientific Inc.

2.2. Human osteosarcoma cell lines

The human OS cell lines 143B (CRL-8303) and MG-63 (CRL-1543) were purchased from American Type Culture Collection (Manassas, VA, USA). Both 143B and MG-63 cells were grown in RPMI 1640 medium supplemented with 10% fetal bovine serum, at 37°C in a

humidified atmosphere containing 5% carbon dioxide. Cells in the logarithmic growth phases were used for the experiments.

2.3. Production of miR-34a prodrug

Recombinant miR-34a prodrug (tRNA/mir-34a) was produced through bacterial fermentation and purified by fast protein liquid chromatograph (FPLC) method to a high degree of homogeneity, as described [30, 31, 33]. The purity of bioengineered tRNA/mir-34a was determined by denaturing urea (8 M) polyacrylamide (8%) gel electrophoresis (PAGE) and verified by a high performance liquid chromatography assay [30], and recombinant tRNA/mir-34a over 98% purity were used in this study.

2.4. Cytotoxicity assay and assessment of synergism and dose-response relationship

The Chou-Talalay approach [38] was employed to critically evaluate if there were synergistic effects between doxorubicin and tRNA/mir-34a in the suppression of human OS 143B (Figure 2) and MG-63 (Figure 3) cell proliferation. Briefly, cells were seeded in 96-well plates (Corning, New York, USA) at 5×10^3 cells per well in 200 μ l media, and treated with Lipofectamine 2000 carried tRNA/mir-34a (0, 0.03, 0.1, 0.3, 1.0, 3.0, 10, 30 nM), or doxorubicin (0, 3, 10, 30, 100, 300, 1,000, 3,000 nM), or their combination (0, 0.03 nM tRNA/mir-34a plus 3 nM doxorubicin, 0.1 nM tRNA/mir-34a plus 10 nM doxorubicin, 0.3 nM tRNA/mir-34a plus 30 nM doxorubicin, 1.0 nM tRNA/mir-34a plus 100 nM doxorubicin, 3.0 nM tRNA/mir-34a plus 300 nM doxorubicin, 10 nM tRNA/mir-34a plus 1,000 nM doxorubicin, 30 nM tRNA/mir-34a plus 3,000 nM doxorubicin). To identify an optimal drug administration Schedule, four different Schedules (Figures 2-3) were tested. Schedule 1: tRNA/mir-34a was administered on day 1, and doxorubicin was given on day 2; Schedule 2: both tRNA/mir-34a and doxorubicin were administered on day 1; Schedule 3: doxorubicin was administered on day 1, and tRNA/mir-34a was given on day 2; Schedule 4: both tRNA/mir-34a and doxorubicin were administered on day 2. Cell viability was determined using MTT assay at 72 h post-treatment, as described [30, 31, 33].

The degrees of inhibition of cell proliferation by various concentrations of treatments were normalized to corresponding vehicle controls which were set as 0% inhibition. To estimate pharmacodynamic parameters (e.g., EC50, Hill slope, Top and Bottom values), the anti-proliferation data for tRNA/mir-34a were fitted to an inhibitory dose-response model with variable slope ($Y = \text{Bottom} + (\text{Top} - \text{Bottom}) / (1 + 10^{((\text{LogEC50} - X) * \text{HillSlope}))}$); GraphPad Prism, San Diego, CA) since tRNA/mir-34a at the tested concentrations showed a partial inhibition. By contrast, the anti-proliferation data for doxorubicin and tRNA/mir-34a plus doxorubicin combination were fitted to an inhibitory, normalized dose-response model with variable slope ($Y = 100 / (1 + 10^{((\text{LogEC50} - X) * \text{HillSlope}))}$); GraphPad Prism) because these agents at the tested concentrations showed a full inhibition.

To define the synergism for the combinations, drug combination index (CI) values at each fraction affected (Fa) [38] (Figures 2-3) were calculated with CompuSyn software (ComboSyn, Inc., USA). $CI < 1$ indicates synergism, $CI = 1$ indicates additivity, and $CI > 1$ indicates antagonism between the two drugs.

2.5. Apoptosis and cell cycle analyses

Human OS 143B cells were seeded in six-well plates at a density of 0.1×10^6 cells per well and treated with 4 nM tRNA/mir-34a, or 60 nM doxorubicin, or 4 nM tRNA/mir-34a plus 60 nM doxorubicin, or vehicle for 48 h. To investigate the effects on apoptosis, cells were incubated with Annexin V-FITC conjugate and propidium iodide solution (Trevigen Inc., Gaithersburg, MD, USA). To assess the impact on cell cycle, DNAs of the cells were stained with PI/RNase Staining Buffer (BD Biosciences). Samples were analyzed on a FACS Canto flow cytometer (BD Biosciences), and all data were analysed by Flowjo (Ashland, OR, USA). Cells were treated in triplicate and assayed separately.

2.6. Cell invasion assay

Human OS 143B cells were seeded in six-well plates and treated with 4 nM tRNA/mir-34a, or 60 nM doxorubicin, or 4 nM tRNA/mir-34a plus 60 nM doxorubicin, or vehicle. After 72 h, cells were collected and 3×10^4 cells were subjected to invasion assay using the Corning BioCoat Matrigel Invasion Chamber coated with 8.0 μm PET membrane (Corning, NY, USA) for 24 h. The upper inserts with matrigel coating were then fixed with 10% formalin, stained with 0.1% crystal violet, and photographed under an Olympus IX2-UCB microscope (200 \times magnification). Cells were treated in triplicate and assayed separately. Five fields per insert were photographed, and the numbers of invaded cells were counted using Adobe Photoshop's count tool and compared between different treatments.

2.7. RNA isolation and reverse transcription quantitative real-time PCR (RT-qPCR)

Human OS 143B cells were treated with 4 nM tRNA/mir-34a, 60 nM doxorubicin, or combination of 4 nM tRNA/mir-34a and 60 nM doxorubicin, or vehicle control. Cells were harvested at 72 h post-treatment, and total RNAs were isolated using a Direct-zol RNA MiniPrep kit (Zymo Research, Irvine, CA, USA). Reverse transcription RT-qPCR analyses were performed using NxGen M-MuLV reverse transcriptase (Lucigen, Middleton, WI, USA), quantitative RT-PCR Master mix (New England Biolabs) on a CFX96 Touch real-time PCR system (Bio-Rad), with gene specific primers as described recently [30, 31, 39]. Cells were treated in triplicate and assayed separately. Relative pre-miR-34a and mature miR-34a levels were calculated by using the comparative threshold cycle (Ct) method with the formula 2^{-Ct} .

2.8. Protein isolation and Western blot analyses

Human OS 143B cells were treated with 4 nM tRNA/mir-34a, 60 nM doxorubicin, or combination of 4 nM tRNA/mir-34a and 60 nM doxorubicin, or vehicle control. Cells were harvested at 72 h post-treatment with trypsin and washed twice with cold PBS. Cell lysates were prepared using RIPA buffer (Rockland Immunochemical Inc., Limerick, PA, USA) supplemented with the complete protease inhibitor cocktail (Roche, Nutley, NJ, USA), and protein concentrations were determined using a BCA Protein Assay Kit (Thermo Fisher Scientific Inc.). Whole cell proteins (40 $\mu\text{g}/\text{lane}$) were separated on a 10% SDS-PAGE gel and transferred onto PVDF membranes using a Trans-Blot Turbo Transfer System (Bio-Rad). Membranes were incubated with anti-SIRT1 (1:500 dilution; H-300; Santa Cruz Biotech Inc., Texas, TX), anti-c-MET (1:200; C-28; Santa Cruz), anti-CDK6 (1:1000; C-21;

Santa Cruz), or anti-GAPDH (1:2,000; FL-335; Santa Cruz) rabbit polyclonal antibody, and then with a peroxidase goat anti-rabbit IgG (Jackson ImmunoResearch Inc., West Grove, PA). After incubated with Clarity Western ECL substrates (Bio-Rad), the proteins were visualized with the ChemiDoc MP Imaging System (Bio-Rad). Band density was determined by Image Lab software (Bio-Rad), and GAPDH was used as a loading control.

2.9. Efficacy and safety of combination therapy in orthotopic osteosarcoma xenograft tumor mouse model

All animal procedures were approved by the Institutional Animal Care and Use Committee (IACUC) at UC-Davis, and were conducted in accordance with the Guide for the Care and Use of Laboratory Animals issued by the National Institutes of Health. Athymic nude mice (4- to 6-week old males, J:NU strain) were purchased from The Jackson Laboratory (Bar Harbor, ME, USA). Orthotopic OS xenograft tumors were established through subperiosteal injection of OS cells [28, 40]. Briefly, 143B cells (4-6 passages) were suspended in PBS to a final concentration of 3×10^7 cells/ml, and 50 μ l of the cell suspension (1.5×10^6 cells) were mixed with 50 μ l of matrigel matrix (BD Biosciences). 100 μ l of the above cell suspension were injected subperiosteally using a 25 gauge needle (BD Biosciences) onto the right proximal lateral tibia of each mouse anesthetized i.p. with ketamine (80 mg/kg) and xylazine (7 mg/kg). Gentle pressure was applied to the injection site for 10 sec to prevent the cells from oozing out. The injection sites were disinfected afterward.

On day 9 post-inoculation, 24 mice showing similar body weights and tumor sizes were randomly divided into 4 groups (6 mice per group). Each mouse in Group 1 was treated i.v. via tail vein with a loading dose of doxorubicin (60 μ g) plus tRNA/mir-34a (20 μ g) formulated with *in vivo*-jetPEI (Polyplus-transfection Inc., New York, NY) on Day 9, followed by five maintenance doses (30 μ g doxorubicin and 10 μ g tRNA/mir-34a) in two weeks. Doses were chosen according to those reported previously [30, 41] and assessed in our pilot study. Mice in Group 2 were treated only with identical doses of doxorubicin, and mice in Group 3 were administered only with tRNA/mir-34a. Mice in Group 4 were treated with drug vehicle.

Tumor size was measured with a caliper, and tumor volume was calculated using the equation: tumor volume (mm^3) = (length + width) (mm) \times length (mm) \times width (mm) \times 0.2618) [42]. On Day 22 post-inoculation, all mice were sacrificed and tumors were dissected and weighed. Tumors were fixed in 10% formalin and subjected to hematoxylin and eosin staining histological examination in the Clinical Immunohistochemistry Laboratory at Roswell Park Cancer Institute. In addition, blood sample was collected, and serum was isolated using a serum separator (BD Biosciences) and then subjected to blood chemistry profiling in the Comparative Pathology Laboratory at UC-Davis.

2.10. Statistical analysis

Values were expressed as mean \pm SD. Depending upon the numbers of groups and variances, data were analyzed using one-way or two-way ANOVA with Bonferroni post-tests (GraphPad Prism). Difference was considered as statistically significant when the probability was less than 0.05 ($P < 0.05$).

3. Results

3.1. Co-administration of bioengineered miR-34a prodrug and doxorubicin synergistically inhibits osteosarcoma cell proliferation, and the best outcomes can be achieved when cells are treated at earlier stage

To critically assess whether miR-34a prodrug and doxorubicin produce synergistic effects in the suppression of OS cancer cell proliferation, we conducted combination analysis using Chou-Talalay method [38]. Our data showed that single drug treatment and all the four different Schedules of combination treatments exhibited dose-dependent antiproliferative effects against human OS 143B (Figure 2A-D) and MG63 (Figure 3A-D) cells. The synergism between doxorubicin and miR-34a prodrug was indicated by the drug combination index (CI) values (less than 1) at various inhibitory levels (Figure 2E and 3E). The maximal synergistic effects showing the lowest CI values at all inhibition levels were identified for Schedule 2 treatment (Figure 2E), in which doxorubicin and bioengineered miR-34a prodrug were administered together to the cells on Day 1. The results indicate that optimal outcomes may be achieved when human carcinoma cells are subjected to combination therapy at earlier stage.

The Schedule 2 combination as an optimal treatment is also manifested by the estimated pharmacodynamic parameters including EC₅₀ (potency) and Top (efficacy) values (Figure 2F and Figure 3F). Although monotherapy with miR-34a prodrug showed the highest potency against OS cells, as indicated by the lowest EC₅₀ values (< 5 nM), only a partial inhibition (40-70%) was achieved. On the other hand, doxorubicin monotherapy was able to produce the maximal efficacy (100%), whereas it was relatively less potent (EC₅₀ > 50 nM). By contrast, the Schedule 2 combination therapy with miR-34a prodrug and doxorubicin exerted the maximal efficacy (100%) and high potency (EC₅₀ = 8 nM). In addition, the 143B cells that carry a *p53* mutant and show a high level of *p53* expression for broad applications to OS cancer biology and new therapies [40, 42-44] were more sensitive to the Schedule 2 combination therapy (Figure 2F) than MG-63 cells (Figures 3F), which the latter consist of wild-type *p53* and lower level of *p53* expression and may [26, 45, 46] or may not be tumorigenic [43]. Therefore, only 143B cells and Schedule 2 combination were utilized for the following *in vitro* mechanistic and *in vivo* therapeutic studies.

3.2. Combination treatment with miR-34a prodrug and doxorubicin largely enhances late apoptosis and necrosis in osteosarcoma 143B cells

To assess whether the suppression of 143B cell proliferation involves apoptosis mechanism, we determined apoptotic profiles through Annexin V/propidium iodide flow cytometric analyses of cells at 48 h post-treatment (Figure 4). The data showed that tRNA/miR-34a treatment mainly induced an early apoptosis, as compared to vehicle control ($P < 0.01$, two-way ANOVA). Doxorubicin treatment not only caused an early apoptosis ($P < 0.01$) but also induced late apoptosis to a significantly higher level ($P < 0.001$). In contrast, combination treatment with tRNA/miR-34a and doxorubicin led to a strikingly high level of necrosis ($P < 0.001$) in 143B cells, in addition to a comparable level of early apoptosis and much greater degree of late apoptosis ($P < 0.05$; compared to single drug treatment). The results demonstrate that treatment of osteosarcoma 143B cells with miR-34a prodrug and

doxorubicin combination amplifies the effects of single drug treatment towards much greater levels of late apoptosis and necrosis.

3.3. Combination treatment with doxorubicin and genetically engineered miR-34a prodrug induces an extensive G2 cell cycle arrest in osteosarcoma 143B cells

To investigate how cell cycle is affected by each drug treatment, we measured the cell cycle profiles through flow cytometric analysis of propidium iodide-stained cells at 48 h post-treatment (Figure 5). Compared to vehicle treatment, both tRNA/mir-34a and doxorubicin treatment alone led to approximately 90% higher accumulation of 143B cells in G2 phase ($P < 0.01$, two-way ANOVA). When 143B cells were subjected to combination treatment with tRNA/mir-34a and doxorubicin, even greater portions of cells were arrested in G2 cell cycle, e.g., 120% more than either tRNA/mir-34a or doxorubicin treatment ($P < 0.001$). Such a striking G2 phase arrest induced by combination treatment was also accompanied by a significant reduction of cells in G1 and S phases, as compared with single drug or vehicle treatment ($P < 0.001$). The results suggest that the stronger antiproliferative activity of combination treatment against OS 143B cells (Figure 2) involves more extensive G2 cell cycle arrest.

3.4. Combination treatment with miR-34a prodrug and doxorubicin inhibits the invasion capability of human 143B cells to a much greater degree than single drug alone

We further carried out Matrigel invasion assays to compare the effects of single drug and combination treatment on cell invasion capability (Figure 6) because cancer cell invasion represents a critical process for tumor progression and metastasis. The data showed that the invasion ability of 143B cells treated with tRNA/mir-34a ($P < 0.01$, one-way ANOVA) and doxorubicin ($P < 0.001$) alone was reduced by 25% and 60%, respectively, as compared to the vehicle control. Furthermore, combination treatment with tRNA/mir-34a and doxorubicin inhibited the invasion ability by 85%, a significantly greater degree than tRNA/mir-34a ($P < 0.001$) or doxorubicin ($P < 0.05$) alone. The results indicate that combination treatment is much more effective than single drug treatment to inhibit the invasion ability of human OS 143B cells.

3.5. Doxorubicin slightly elevates miR-34a level in osteosarcoma cells and bioengineered miR-34a prodrug is readily processed to a high level of mature miR-34a, which leads to a lower protein level of miR-34a targeted (proto-)oncogene

To understand the molecular mechanisms behind miR-34a prodrug and combination treatment in the modulation of 143B cellular processes, we determined the protein levels of a number of miR-34a targeted (proto-)oncogenes after the measurement of pre-miR-34a and mature miR-34a levels (Figure 7). Consistent with previous findings [47], doxorubicin was able to elevate cellular pre-miR-34a and mature miR-34a levels by certain levels, as compared with vehicle control. OS 143B cells treated with tRNA/mir-34a showed 383-fold higher pre-miR-34a levels and 117-fold higher mature miR-34a concentrations, agreeing with our recent findings from human lung carcinoma cells [30]. Furthermore, compared with vehicle treatment, tRNA/mir-34a significantly reduced the protein levels of CDK6 and c-MET, while doxorubicin showed no or minor effects (Figure 6C-D). Interestingly, combination treatment with doxorubicin and tRNA/mir-34a led to even higher levels of

mature miR-34a (143-fold) in the cells, which also caused a significantly lower level of SIRT1, CDK6 and c-MET than vehicle or doxorubicin treatment (Figure 6C-D). The results suggest that the more effective modulation of OS cellular processes by combination treatment with bioengineered miR-34a prodrug and doxorubicin (Figures 2-5) may be partially attributable to the higher levels of mature miR-34a and greater extents of suppression of miR-34a targeted (proto-)oncogene (e.g., SIRT1) expression (Figure 7).

3.6. Combination therapy with bioengineered miR-34a prodrug and doxorubicin is more effective than single drug to control osteosarcoma growth in an orthotopic xenograft tumor mouse model

We then investigated the efficacy of combination therapy versus monotherapy *in vivo* after establishing an orthotopic OS xenograft tumor mouse model (Figure 8). While systemic administration of miR-34a prodrug or doxorubicin monotherapy showed a significant suppression ($P < 0.001$, two-way ANOVA; Figure 8B) of the outgrowth of viable tumors than vehicle control, combination therapy was able to reduce tumor growth to a significantly greater degree than the single drug treatment ($P < 0.01$, Figure 8B). This is also indicated by visual inspection of the sizes (Figure 8C) and quantitative measurement of weights (Figure 8D) of dissected xenograft tumors. In addition, xenografts dissected from mice under combination therapy had much more severe tumor necrosis (Figure 8E) than those under monotherapy, as revealed by histological examination. Together, these results indicate that combination therapy with miR-34a prodrug and doxorubicin is more effective than monotherapy in suppressing OS xenograft tumor growth *in vivo*.

3.7. Systemically co-administered, multiple doses of miR-34a prodrug and doxorubicin are relatively safe to athymic mice

Compared with vehicle control or monotherapy, combination therapy with tRNA/miR-34a and doxorubicin did not alter mouse body weights (data not shown) or cause any signs of stress such as hunched posture and labored movement. In addition, we examined blood chemistry profiles to evaluate if combination therapy with bioengineered miR-34a prodrug and doxorubicin altered mouse liver and kidney functions (Figure 9). Although alanine aminotransferase (ALT) concentrations in mice under combination therapy were elevated to a statistically significant higher level ($P < 0.05$, one-way ANOVA), as compared to vehicle control, the altered ALT concentrations were still lower than 90 U/L and might not indicate any severe hepatic toxicity. In addition, none of other blood biomarkers including aspartate aminotransferase (AST), total protein, albumin, total bilirubin, alkaline phosphatase (ALP), blood urea nitrogen (BUN), and creatinine was significantly altered by combination therapy (Figure 9), indicating the absence of hepatic and renal toxicity. These results suggest that therapeutic doses of miR-34a prodrug and doxorubicin co-administered intravenously are relatively safe in the orthotopic OS xenograft tumor mouse models.

4. Discussion

Given the fact that miR-34a exhibits antiproliferative activity via RNA interference and doxorubicin exerts anticancer activity through DNA intercalation, it was reasoned that combination therapy with miR-34a and doxorubicin could produce synergistic effects. Using

Chou-Talalay approach [38], our comprehensive studies clearly demonstrated a synergism between doxorubicin and bioengineered miR-34a prodrug for the inhibition of human OS cell proliferation, which were attributable to much greater degrees of late apoptosis and necrosis, G2 cell cycle arrest, and suppressed expression of several target (proto-)oncogenes. In addition, bioengineered miR-34a prodrug and doxorubicin co-administered intravenously was more effective than single drug treatment for the control of orthotopic OS xenograft tumor growth in mouse models.

Research and development of miRNA-based mono- and combination therapies primarily utilizes synthetic miRNA mimics or precursors. In contrast to natural RNAs that may consist of posttranscriptional modifications on the nucleobases, synthetic miRNA agents are comprised of extensive artificial modifications on the ribose rings and phosphate bones and may have different tertiary structures, physicochemical properties, biological activities, and/or safety profiles [32]. The present study defined the efficacy and safety profiles of genetically engineered miR-34a prodrug in the control of OS *in vitro* and *in vivo*, which is a natural RNA agent produced and folded in live cells [30, 31]. In addition, bioengineered miR-34a prodrug is distinguished from viral or non-viral vector-based miR-34a expression plasmids/systems that are rather DNA agents and thus could complicate RNA-based processes [32].

The finding on an optimal antiproliferative effect for Schedule 2 combination treatment was rather unexpected but reasonable because the order of drug administration may have a dramatic impact on therapeutic outcomes. Many reports including ours [33, 48, 49] on the alteration of chemosensitivity by co-administered miRNA/siRNA agents involve the pre-treatment with miRNA/siRNA drugs before chemotherapy. The present study, however, showed that simultaneous treatment of cancer cells with miR-34a prodrug and doxorubicin at earlier stage (Schedule 2) offered the best outcomes, which were clearly demonstrated by the greater degrees of potency (ED50 values) and efficacy (Top) as well as the strongest synergism (CI values). Schedule 2 combination as the best treatment may be explained by the fact that human carcinoma cells are more sensitive to drugs at lower degrees of confluence [50]. Therefore, our findings support the notion to utilize safe doses of combination therapies to simultaneously treat cancers as soon as possible, which was also implemented in our therapy study in xenograft tumor mouse models. Overall our *in vitro* and *in vivo* studies on OS using novel bioengineered miR-34a prodrug [30] agree with previous findings that combination therapy with miR-34a and doxorubicin works better than single drug for the treatment of breast [23] and colorectal cancer [51], which focus more on new drug delivery systems.

It has been shown that miR-34a controls human carcinoma cell growth by inducing apoptosis and cell cycle arrest [19, 21]. Likewise, doxorubicin is able to induce apoptosis and cell cycle arrest at specific doses and under particular conditions [52]. Results from the present study support such mechanistic actions of miR-34a and doxorubicin in the regulation of OS cellular processes. Most importantly, our studies demonstrated that combination treatment with miR-34a and doxorubicin provoked much greater degrees of late apoptosis and necrosis as well as G2 cell cycle arrest, in accordance with the synergistic effects in suppressing OS cell proliferation. In addition, doxorubicin was able to elevate miR-34a

levels in OS cells while bioengineered tRNA/mir-34a agents were selectively processed to large quantities of mature miR-34a. These results are consistent with previous findings on a p53-dependent induction of miR-34a by doxorubicin in human colon cancer cells [47] and efficient production of mature miR-34a from tRNA/mir-34a in human lung cancer cells [30, 31], respectively. Subsequently, protein levels of several well-characterized miR-34a target (proto-)oncogenes including SIRT1, CDK6, and c-MET [18-21] were much lower in OS cells co-administered with miR-34a prodrug and doxorubicin, providing a molecular explanation for the impact of combination treatment on OS cell proliferation, apoptosis, cell cycle arrest, and invasion ability.

The 143B cells consisting of a p53 mutant and high-level expression of p53 commonly found in human malignant OS are proper models for studying OS biology and exploring new therapies [40, 42-44]. Therefore, the 143B cells were employed to produce orthotopic OS xenograft tumors in mouse models to evaluate the efficacy of combination therapy *in vivo*. Our study revealed a significant suppression of OS xenograft tumor growth by single drug treatment, compared to the vehicle control. Moreover, our data showed a much greater degree of suppression of 143B xenografts by combination therapy than single drug treatment, which was associated with more severe tumor necrosis. The improved therapeutic outcomes from combination treatment are also consistent with the synergism between miR-34a prodrug and doxorubicin chemotherapy identified in 143B cells *in vitro*. In addition, while combination therapy tended to alter serum ALT concentrations and it reached statistically significant ($P = 0.02$), the changed ALT concentrations were still quite low (< 90 U/L) and might not indicate severe hepatic toxicity. Because all other biomarkers including AST, bilirubin, albumin, ALP, BUN, creatinine, and total proteins levels were unchanged in the mice, it is concluded that therapeutic doses of bioengineered miR-34a prodrug and doxorubicin were tolerated in tumor-bearing mice and did not cause any toxicity to the liver and kidney. Nevertheless, it is unknown if co-administration of miR-34a prodrug would affect cardiotoxicity of doxorubicin, although lower doses of doxorubicin used in current study unlikely induce any cardiac injury [41, 53]. Therefore, the safety and efficacy of bioengineered miR-34a prodrug plus doxorubicin combination therapy are subjected to further studies using more animal models, dose levels and various assays before clinical investigations.

In summary, the present study demonstrated that systemic co-administration of bioengineered miR-34a prodrug and doxorubicin was more effective than single drug treatment for the control of OS tumor growth in an orthotopic xenograft tumor mouse model. Synergistic effects were obvious for doxorubicin and miR-34a prodrug combination in the inhibition of osteosarcoma cell proliferation *in vitro*, and the best outcomes were achieved when both drugs were administered simultaneously to the cells at early stage. The synergistic antiproliferative activity was mechanistically explained by a much greater degree of late apoptosis, necrosis, and G2 cell cycle arrest as well as suppressed protein levels of miR-34a targeted (proto-)oncogenes. These findings support the development of miR-34a replacement therapy plus and doxorubicin chemotherapy combination to combat malignant OS, in which bioengineered miR-34a prodrug represents a new and natural agent for RNA interference.

Acknowledgements

A-X Yu is supported by the Outstanding Medical Academic leader Program of Hubei Province. A-M Yu is supported by NIH grants numbers U01CA175315 and R41AA024029. Y Zhao is funded by the Chinese Scholarship Council (No. 201406270084). The authors appreciate the access to shared resources funded by the UC Davis Comprehensive Cancer Center Support Grant (CCSG) awarded by the National Cancer Institute (NCI P30CA093373) and thank Drs. Hongyong Zhang, Wenwu Xiao, and Tsung-Chieh Shih for their technical help.

Abbreviations

OS	osteosarcoma
miR or miRNA	microRNA
ncRNA	noncoding RNA
miR-34a	MicroRNA-34a
pre-miR-34a or mir-34a	pre-microRNA-34a
tRNA/mir-34a	transfer RNA fusion pre-miR-34a
CDK6	cyclin-dependent kinase 6
c-MET	hepatocyte growth factor receptor
SIRT1	sirtuin-1
RT-qPCR	reverse transcription quantitative real-time PCR

References

- Gorlick R, Janeway K, Lessnick S, Randall RL, Marina N. Committee COGBT. Children's Oncology Group's 2013 blueprint for research: bone tumors. *Pediatr Blood Cancer*. 2013; 60:1009–15. [PubMed: 23255238]
- Rivera-Valentin RK, Zhu L, Hughes DP. Bone Sarcomas in Pediatrics: Progress in Our Understanding of Tumor Biology and Implications for Therapy. *Paediatr Drugs*. 2015; 17:257–71. [PubMed: 26002157]
- Mirabello L, Troisi RJ, Savage SA. Osteosarcoma incidence and survival rates from 1973 to 2004: data from the Surveillance, Epidemiology, and End Results Program. *Cancer*. 2009; 115:1531–43. [PubMed: 19197972]
- Kager L, Zoubek A, Potschger U, Kastner U, Flege S, Kempf-Bielack B, et al. Primary metastatic osteosarcoma: presentation and outcome of patients treated on neoadjuvant Cooperative Osteosarcoma Study Group protocols. *J Clin Oncol*. 2003; 21:2011–8. [PubMed: 12743156]
- Bacci G, Rocca M, Salone M, Balladelli A, Ferrari S, Palmerini E, et al. High grade osteosarcoma of the extremities with lung metastases at presentation: treatment with neoadjuvant chemotherapy and simultaneous resection of primary and metastatic lesions. *J Surg Oncol*. 2008; 98:415–20. [PubMed: 18792969]
- Brennecke P, Arlt MJ, Campanile C, Husmann K, Gvozdenovic A, Apuzzo T, et al. CXCR4 antibody treatment suppresses metastatic spread to the lung of intratibial human osteosarcoma xenografts in mice. *Clin Exp Metastasis*. 2014; 31:339–49. [PubMed: 24390633]
- Cassinelli G, Lanzi C, Tortoreto M, Cominetti D, Petrangolini G, Favini E, et al. Antitumor efficacy of the heparanase inhibitor SST0001 alone and in combination with antiangiogenic agents in the treatment of human pediatric sarcoma models. *Biochemical pharmacology*. 2013; 85:1424–32. [PubMed: 23466421]
- Teicher BA. Searching for molecular targets in sarcoma. *Biochemical pharmacology*. 2012; 84:1–10. [PubMed: 22387046]

9. Ambros V. The functions of animal microRNAs. *Nature*. 2004; 431:350–5. [PubMed: 15372042]
10. Bartel DP. MicroRNAs: target recognition and regulatory functions. *Cell*. 2009; 136:215–33. [PubMed: 19167326]
11. Yu AM. Role of microRNAs in the regulation of drug metabolism and disposition. *Expert Opin Drug Metab Toxicol*. 2009; 5:1513–28. [PubMed: 19785514]
12. Bader AG, Brown D, Winkler M. The promise of microRNA replacement therapy. *Cancer research*. 2010; 70:7027–30. [PubMed: 20807816]
13. Kasinski AL, Slack FJ. Epigenetics and genetics. MicroRNAs en route to the clinic: progress in validating and targeting microRNAs for cancer therapy. *Nature reviews Cancer*. 2011; 11:849–64. [PubMed: 22113163]
14. Ling H, Fabbri M, Calin GA. MicroRNAs and other non-coding RNAs as targets for anticancer drug development. *Nature reviews Drug discovery*. 2013; 12:847–65. [PubMed: 24172333]
15. Welch C, Chen Y, Stallings RL. MicroRNA-34a functions as a potential tumor suppressor by inducing apoptosis in neuroblastoma cells. *Oncogene*. 2007; 26:5017–22. [PubMed: 17297439]
16. He L, He X, Lim LP, de Stanchina E, Xuan Z, Liang Y, et al. A microRNA component of the p53 tumour suppressor network. *Nature*. 2007; 447:1130–4. [PubMed: 17554337]
17. Tivnan A, Tracey L, Buckley PG, Alcock LC, Davidoff AM, Stallings RL. MicroRNA-34a is a potent tumor suppressor molecule in vivo in neuroblastoma. *BMC cancer*. 2011; 11:33. [PubMed: 21266077]
18. Chang TC, Wentzel EA, Kent OA, Ramachandran K, Mullendore M, Lee KH, et al. Transactivation of miR-34a by p53 broadly influences gene expression and promotes apoptosis. *Molecular cell*. 2007; 26:745–52. [PubMed: 17540599]
19. Sun F, Fu H, Liu Q, Tie Y, Zhu J, Xing R, et al. Downregulation of CCND1 and CDK6 by miR-34a induces cell cycle arrest. *FEBS letters*. 2008; 582:1564–8. [PubMed: 18406353]
20. Liu C, Kelnar K, Liu B, Chen X, Calhoun-Davis T, Li H, et al. The microRNA miR-34a inhibits prostate cancer stem cells and metastasis by directly repressing CD44. *Nature medicine*. 2011; 17:211–5.
21. Yamakuchi M, Ferlito M, Lowenstein CJ. miR-34a repression of SIRT1 regulates apoptosis. *Proceedings of the National Academy of Sciences of the United States of America*. 2008; 105:13421–6. [PubMed: 18755897]
22. Vinall RL, Ripoll AZ, Wang S, Pan CX, deVere White RW. MiR-34a chemosensitizes bladder cancer cells to cisplatin treatment regardless of p53-Rb pathway status. *International journal of cancer Journal international du cancer*. 2012; 130:2526–38. [PubMed: 21702042]
23. Deng X, Cao M, Zhang J, Hu K, Yin Z, Zhou Z, et al. Hyaluronic acid-chitosan nanoparticles for co-delivery of MiR-34a and doxorubicin in therapy against triple negative breast cancer. *Biomaterials*. 2014; 35:4333–44. [PubMed: 24565525]
24. Kelnar K, Peltier HJ, Leatherbury N, Stoudemire J, Bader AG. Quantification of therapeutic miRNA mimics in whole blood from non-human primates. *Analytical chemistry*. 2014; 86:1534–42. [PubMed: 24397447]
25. Wang Y, Jia LS, Yuan W, Wu Z, Wang HB, Xu T, et al. Low miR-34a and miR-192 are associated with unfavorable prognosis in patients suffering from osteosarcoma. *Am J Transl Res*. 2015; 7:111–9. [PubMed: 25755833]
26. Wu X, Zhong D, Gao Q, Zhai W, Ding Z, Wu J. MicroRNA-34a inhibits human osteosarcoma proliferation by downregulating ether a go-go 1 expression. *Int J Med Sci*. 2013; 10:676–82. [PubMed: 23569431]
27. Zhao H, Ma B, Wang Y, Han T, Zheng L, Sun C, et al. miR-34a inhibits the metastasis of osteosarcoma cells by repressing the expression of CD44. *Oncol Rep*. 2013; 29:1027–36. [PubMed: 23314380]
28. Yan K, Gao J, Yang T, Ma Q, Qiu X, Fan Q, et al. MicroRNA-34a inhibits the proliferation and metastasis of osteosarcoma cells both in vitro and in vivo. *PloS one*. 2012; 7:e33778. [PubMed: 22457788]
29. Novello C, Pazzaglia L, Conti A, Quattrini I, Pollino S, Perego P, et al. p53-dependent activation of microRNA-34a in response to etoposide-induced DNA damage in osteosarcoma cell lines not impaired by dominant negative p53 expression. *PloS one*. 2014; 9:e114757. [PubMed: 25490093]

30. Wang WP, Ho PY, Chen QX, Addepalli B, Limbach PA, Li MM, et al. Bioengineering Novel Chimeric microRNA-34a for Prodrug Cancer Therapy: High-Yield Expression and Purification, and Structural and Functional Characterization. *J Pharmacol Exp Ther*. 2015; 354:131–41. [PubMed: 26022002]
31. Chen QX, Wang WP, Zeng S, Urayama S, Yu AM. A general approach to high-yield biosynthesis of chimeric RNAs bearing various types of functional small RNAs for broad applications. *Nucleic acids research*. 2015; 43:3857–69. [PubMed: 25800741]
32. Ho PY, Yu AM. Bioengineering noncoding RNAs for research and development. *Wiley Interdiscip Rev RNA*. in submission.
33. Li MM, Addepalli B, Tu MJ, Chen QX, Wang WP, Limbach PA, et al. Chimeric MicroRNA-1291 Biosynthesized Efficiently in *Escherichia coli* Is Effective to Reduce Target Gene Expression in Human Carcinoma Cells and Improve Chemosensitivity. *Drug metabolism and disposition: the biological fate of chemicals*. 2015; 43:1129–36. [PubMed: 25934574]
34. Tahover E, Patil YP, Gabizon AA. Emerging delivery systems to reduce doxorubicin cardiotoxicity and improve therapeutic index: focus on liposomes. *Anticancer Drugs*. 2015; 26:241–58. [PubMed: 25415656]
35. Schwebe M, Ameling S, Hammer E, Monzel JV, Bonitz K, Budde S, et al. Protective effects of endothelin receptor A and B inhibitors against doxorubicin-induced cardiomyopathy. *Biochemical pharmacology*. 2015; 94:109–29. [PubMed: 25660617]
36. Granados-Principal S, El-Azem N, Pamplona R, Ramirez-Tortosa C, Pulido-Moran M, Vera-Ramirez L, et al. Hydroxytyrosol ameliorates oxidative stress and mitochondrial dysfunction in doxorubicin-induced cardiotoxicity in rats with breast cancer. *Biochemical pharmacology*. 2014; 90:25–33. [PubMed: 24727461]
37. Tarasenko N, Cutts SM, Phillips DR, Berkovitch-Luria G, Bardugo-Nissim E, Weitman M, et al. A novel valproic acid prodrug as an anticancer agent that enhances doxorubicin anticancer activity and protects normal cells against its toxicity in vitro and in vivo. *Biochemical pharmacology*. 2014; 88:158–68. [PubMed: 24463168]
38. Chou TC. Drug combination studies and their synergy quantification using the Chou-Talalay method. *Cancer research*. 2010; 70:440–6. [PubMed: 20068163]
39. Li X, Pan YZ, Seigel GM, Hu ZH, Huang M, Yu AM. Breast cancer resistance protein BCRP/ABCG2 regulatory microRNAs (hsa-miR-328, -519c and -520h) and their differential expression in stem-like ABCG2+ cancer cells. *Biochemical pharmacology*. 2011; 81:783–92. [PubMed: 21219875]
40. Su Y, Wagner ER, Luo Q, Huang J, Chen L, He BC, et al. Insulin-like growth factor binding protein 5 suppresses tumor growth and metastasis of human osteosarcoma. *Oncogene*. 2011; 30:3907–17. [PubMed: 21460855]
41. Ottewell PD, Woodward JK, Lefley DV, Evans CA, Coleman RE, Holen I. Anticancer mechanisms of doxorubicin and zoledronic acid in breast cancer tumor growth in bone. *Molecular cancer therapeutics*. 2009; 8:2821–32. [PubMed: 19789217]
42. Luu HH, Kang Q, Park JK, Si W, Luo Q, Jiang W, et al. An orthotopic model of human osteosarcoma growth and spontaneous pulmonary metastasis. *Clin Exp Metastasis*. 2005; 22:319–29. [PubMed: 16170668]
43. Mohseny AB, Machado I, Cai Y, Schaefer KL, Serra M, Hogendoorn PC, et al. Functional characterization of osteosarcoma cell lines provides representative models to study the human disease. *Lab Invest*. 2011; 91:1195–205. [PubMed: 21519327]
44. Yuan J, Ossendorf C, Szatkowski JP, Bronk JT, Maran A, Yaszemski M, et al. Osteoblastic and osteolytic human osteosarcomas can be studied with a new xenograft mouse model producing spontaneous metastases. *Cancer Invest*. 2009; 27:435–42. [PubMed: 19212826]
45. Ji T, Lin C, Krill LS, Eskander R, Guo Y, Zi X, et al. Flavokawain B, a kava chalcone, inhibits growth of human osteosarcoma cells through G2/M cell cycle arrest and apoptosis. *Molecular cancer*. 2013; 12:55. [PubMed: 23764122]
46. Li B, Yang Y, Jiang S, Ni B, Chen K, Jiang L. Adenovirus-mediated overexpression of BMP-9 inhibits human osteosarcoma cell growth and migration through downregulation of the PI3K/AKT pathway. *Int J Oncol*. 2012; 41:1809–19. [PubMed: 22948234]

47. Tazawa H, Tsuchiya N, Izumiya M, Nakagama H. Tumor-suppressive miR-34a induces senescence-like growth arrest through modulation of the E2F pathway in human colon cancer cells. *Proceedings of the National Academy of Sciences of the United States of America*. 2007; 104:15472–7. [PubMed: 17875987]
48. Pan YZ, Morris ME, Yu AM. MicroRNA-328 negatively regulates the expression of breast cancer resistance protein (BCRP/ABCG2) in human cancer cells. *Mol Pharmacol*. 2009; 75:1374–9. [PubMed: 19270061]
49. Pan YZ, Zhou A, Hu Z, Yu AM. Small nucleolar RNA-derived microRNA hsa-miR-1291 modulates cellular drug disposition through direct targeting of ABC transporter ABCC1. *Drug metabolism and disposition: the biological fate of chemicals*. 2013; 41:1744–51. [PubMed: 23686318]
50. Pelletier H, Millot JM, Chauffert B, Manfait M, Genne P, Martin F. Mechanisms of resistance of confluent human and rat colon cancer cells to anthracyclines: alteration of drug passive diffusion. *Cancer research*. 1990; 50:6626–31. [PubMed: 2208125]
51. Choi KY, Silvestre OF, Huang X, Min KH, Howard GP, Hida N, et al. Versatile RNA interference nanoplatform for systemic delivery of RNAs. *ACS Nano*. 2014; 8:4559–70. [PubMed: 24779637]
52. Lupertz R, Watjen W, Kahl R, Chovolou Y. Dose- and time-dependent effects of doxorubicin on cytotoxicity, cell cycle and apoptotic cell death in human colon cancer cells. *Toxicology*. 2010; 271:115–21. [PubMed: 20346999]
53. Desai VG, J CK, Vijay V, Moland CL, Herman EH, Lee T, et al. Early biomarkers of doxorubicin-induced heart injury in a mouse model. *Toxicol Appl Pharmacol*. 2014; 281:221–9. [PubMed: 25448438]

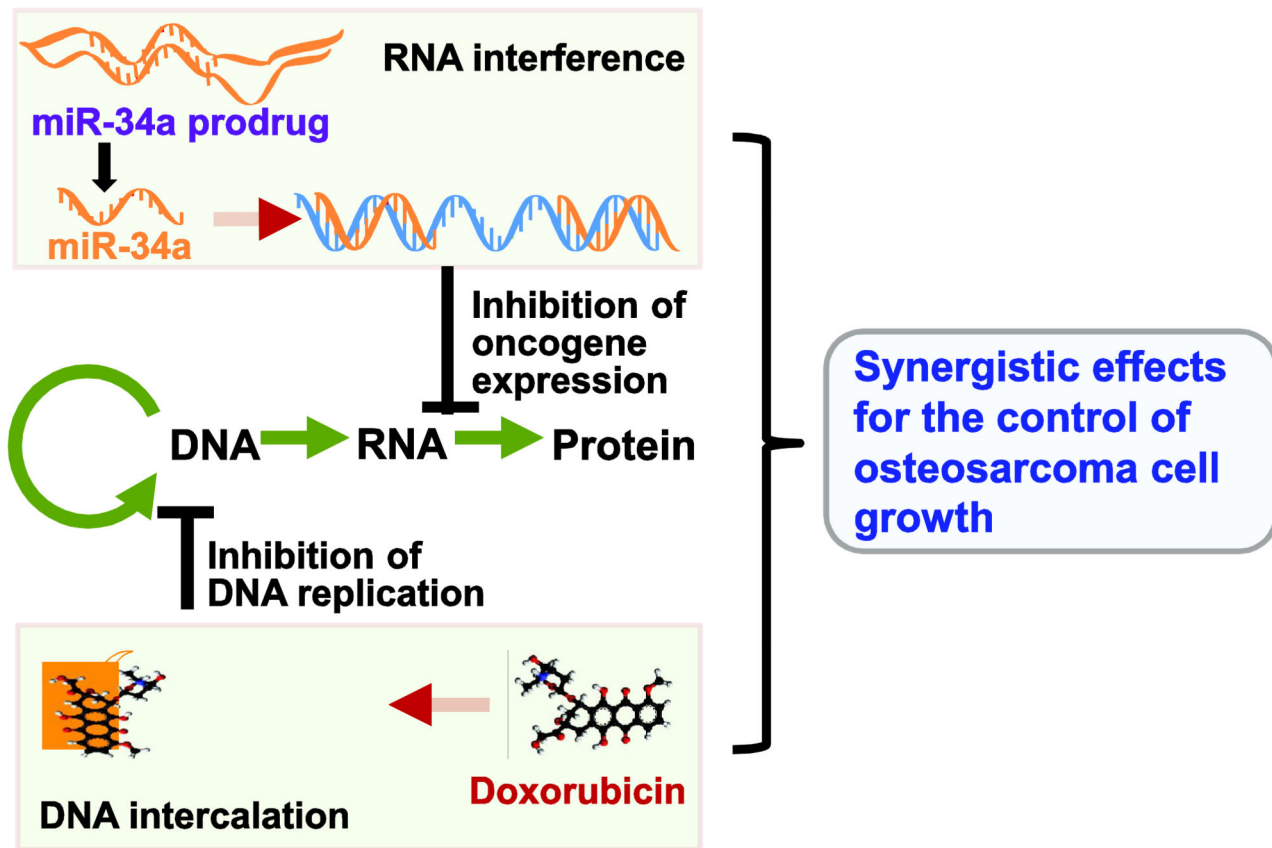


Figure 1. Combination therapy with doxorubicin and miR-34a, which acts through DNA intercalation and RNA interference, respectively, may produce synergistic effects for the control of cancer cell growth.

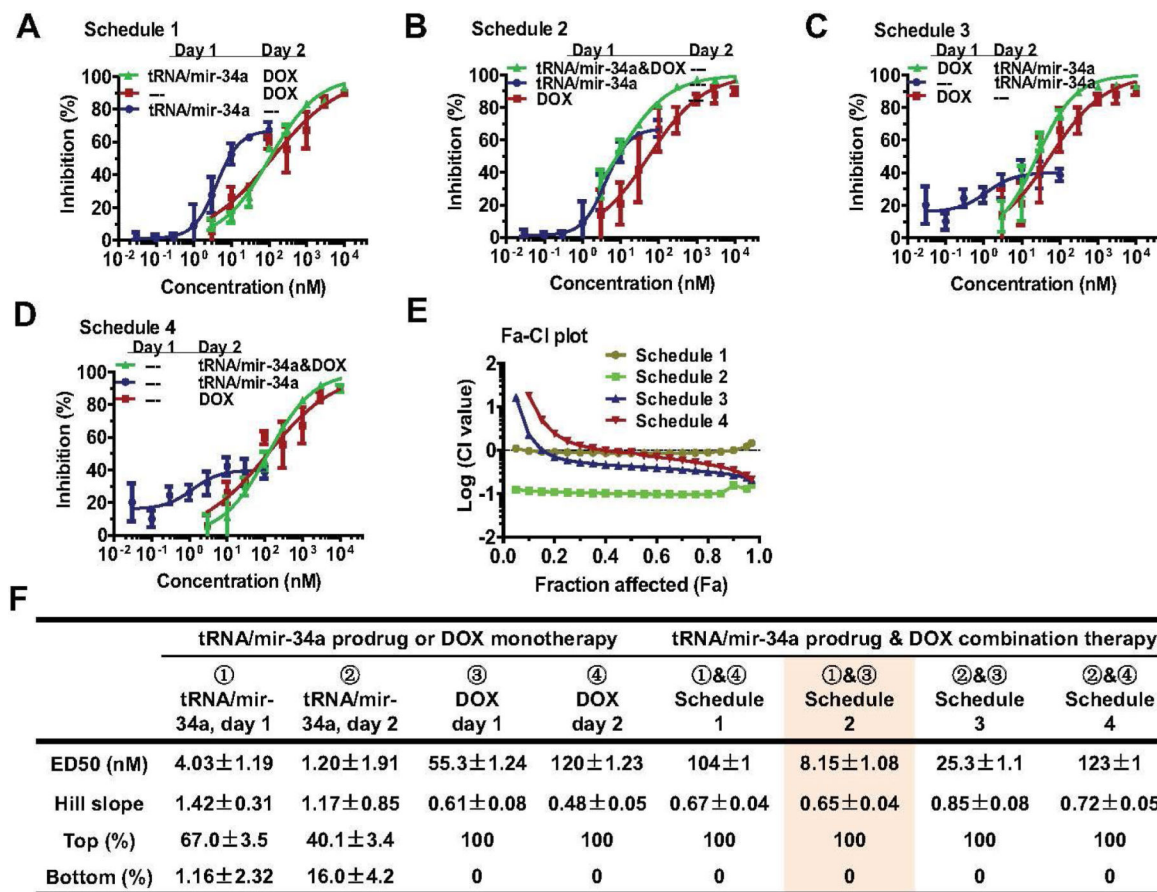


Figure 2. Synergistic effects between bioengineered miR-34a prodrug (tRNA/mir-34a) and doxorubicin (DOX) for the inhibition of osteosarcoma 143B cell proliferation. Cells were treated with various concentrations of tRNA/mir-34a and DOX, alone or in combination. Cell viability was determined using MTT assay at 72 h post-treatment. Dose-response curves were shown for Schedule 1 (A), Schedule 2 (B), Schedule 3 (C), and Schedule 4 (D) treatments versus corresponding controls. (E) Chou-Talalay (Fa-CI) plot demonstrated that Schedule 2 treatment (tRNA/mir-34a plus DOX on Day 1) had the strongest synergistic effects. (F) The estimated pharmacodynamic parameters also revealed Schedule 2 as an optimal treatment. Values are mean ± SD of triplicate treatments.

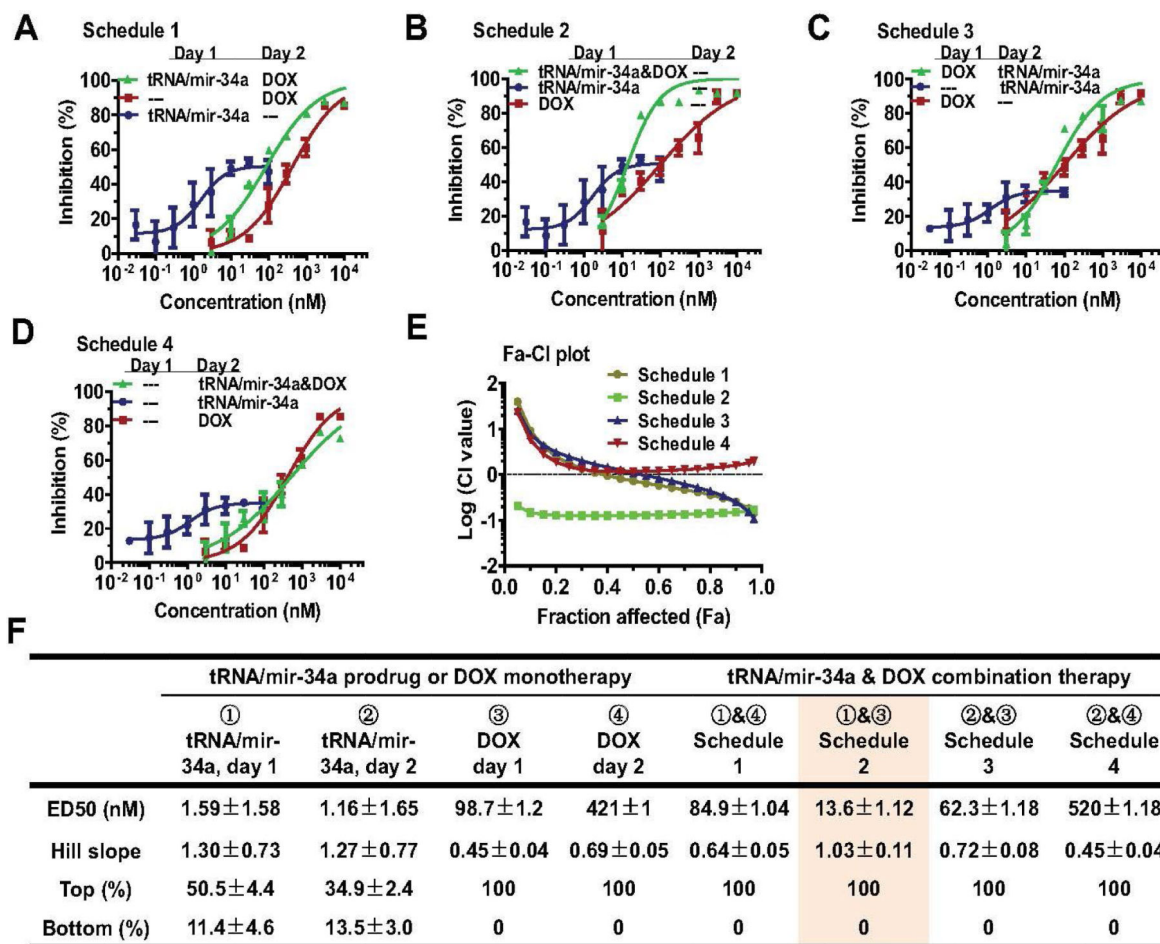


Figure 3. Bioengineered miR-34a prodrug (tRNA/mir-34a) plus doxorubicin (DOX) combination produced synergistic effects against osteosarcoma MG63 cell proliferation. Cells were treated with various concentrations of tRNA/mir-34a and DOX, either alone or in combination, and cell viability was determined using MTT assay after 72 h. Dose-response curves were shown for Schedule 1 (A), Schedule 2 (B), Schedule 3 (C), and Schedule 4 (D) treatments versus corresponding controls. (E) The strongest synergistic effects were revealed for Schedule 2 treatment (tRNA/mir-34a plus DOX on Day 1), as indicated by Chou-Talalay (Fa-CI) plot. (F) The estimated pharmacodynamic parameters also showed that Schedule 2 treatment was optimal. Values are mean ± SD of triplicate treatments.

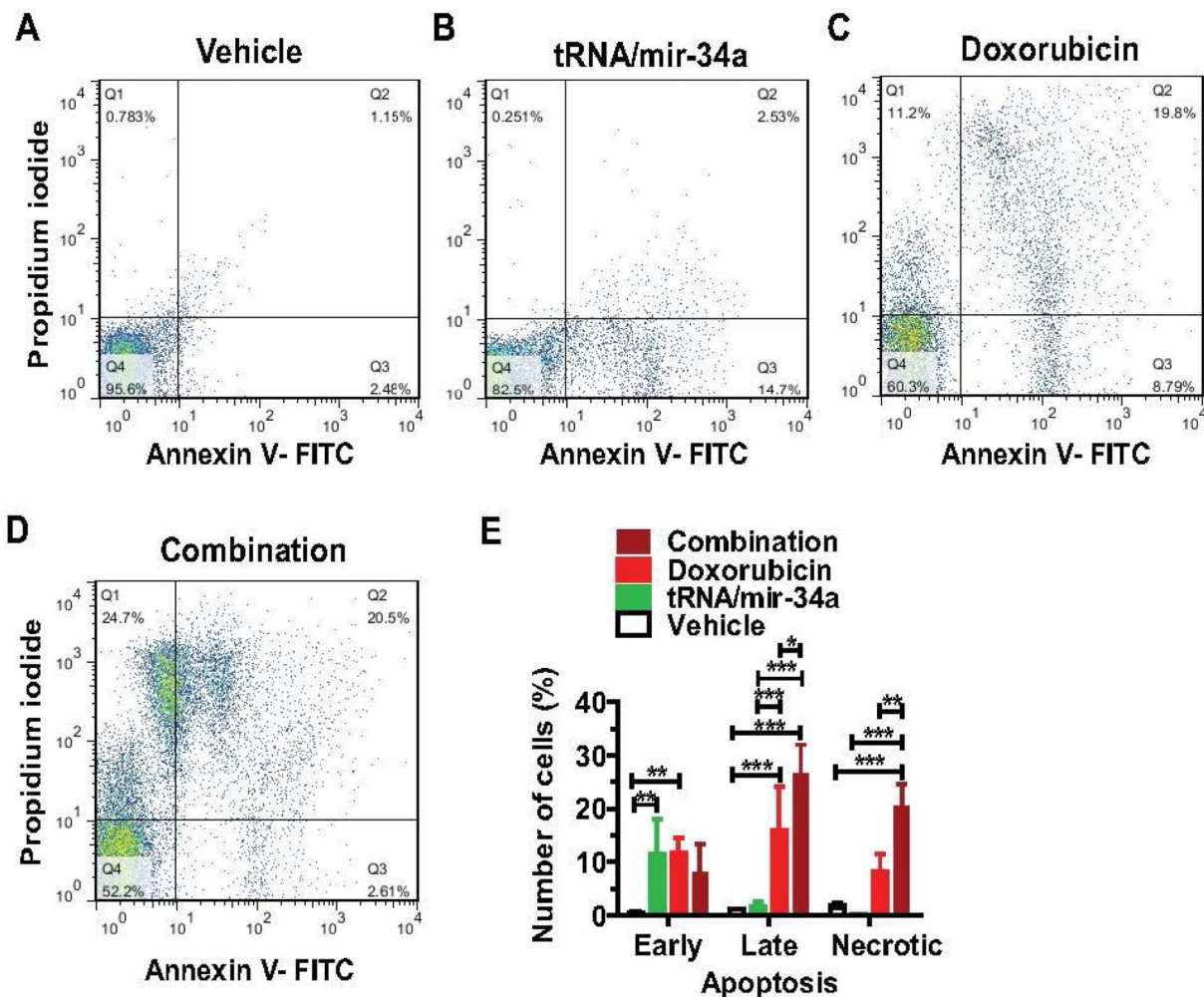


Figure 4. Late apoptosis and necrosis were largely enhanced in osteosarcoma 143B cells treated with bioengineered miR-34a prodrug (tRNA/mir-34a) plus doxorubicin combination, as compared with single drug or vehicle. Comparison of flow cytometry histograms of Annexin V/propidium iodide stained cells, following the treatments with vehicle (A), tRNA/mir-34a (B), doxorubicin (C), and tRNA/mir-34a plus doxorubicin combination (D). (E) Comparison of the percentage of apoptotic cells with different treatments. Values are mean \pm SD of triplicate treatments. * $P < 0.05$, ** $P < 0.01$, and *** $P < 0.001$ (two-way ANOVA).

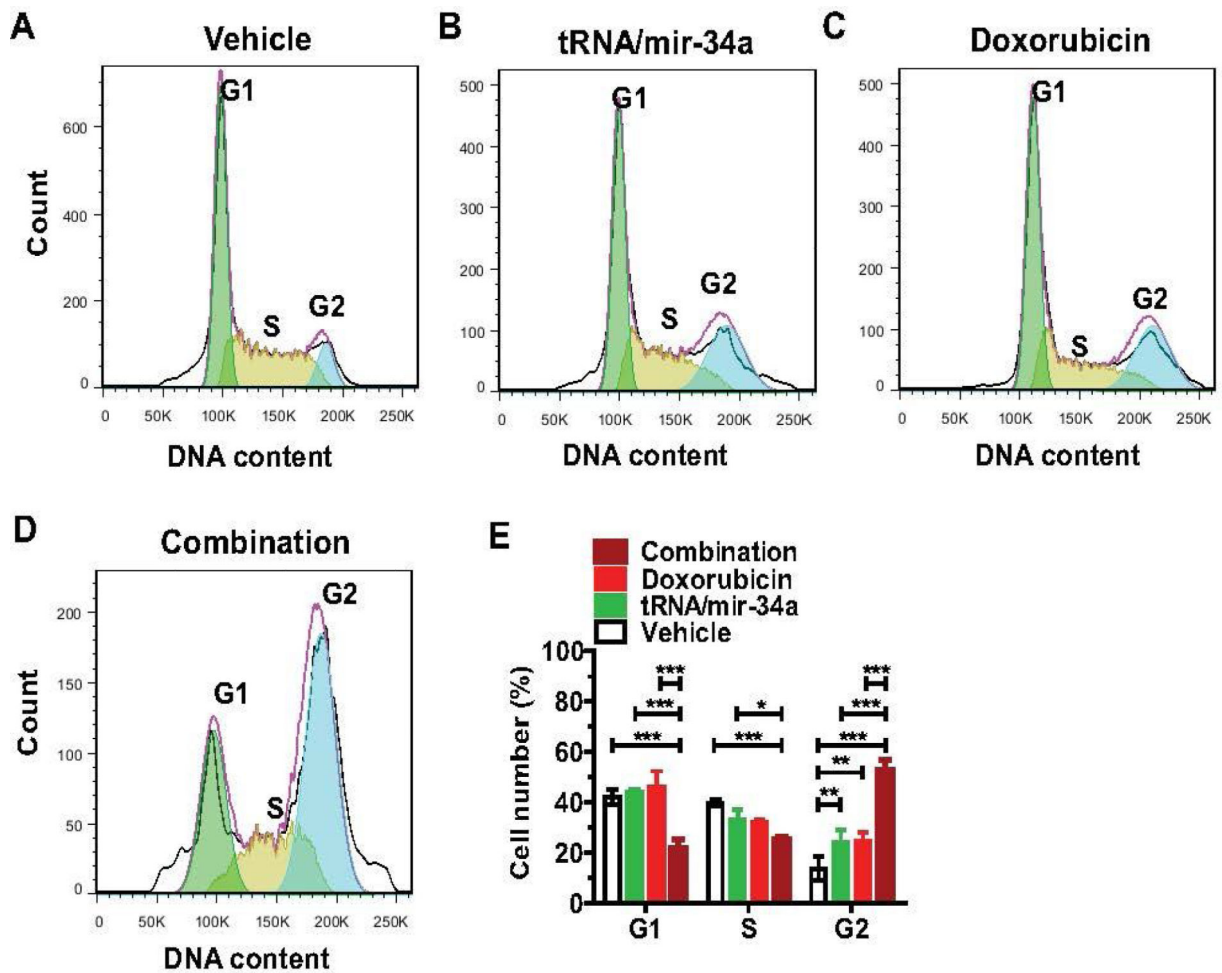


Figure 5. Combination treatment with doxorubicin and genetically engineered miR-34a prodrug induced a much greater degree of G2 cell cycle arrest in osteosarcoma 143B cells than single drug treatment. Comparison of flow cytometry histograms of propidium iodide-stained cells, following the treatments with vehicle (A), tRNA/mir-34a (B), doxorubicin (C), and tRNA/mir-34a plus doxorubicin (D). (E) Comparison of percentage of cells at various phases (G1, S and G2). Values are mean \pm SD of triplicate treatments. *P < 0.05, **P < 0.01, and ***P < 0.001 (two-way ANOVA).

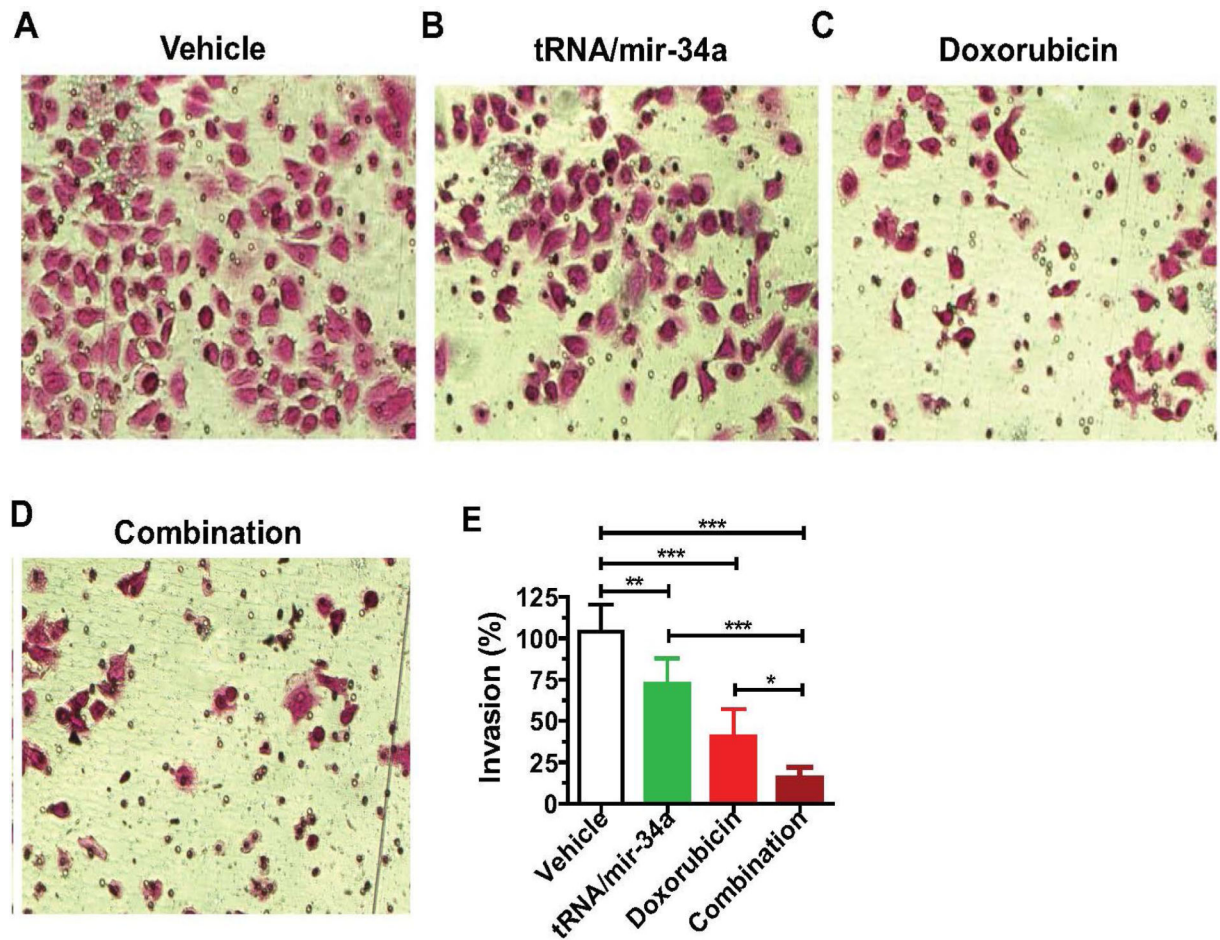


Figure 6.

The invasion capability of human osteosarcoma 143B cells was inhibited to a much greater degree by the combination treatment with doxorubicin and bioengineered miR-34a prodrug than single drug. 72 h post-treatment, cells were subjected to Matrigel invasion assay for 24 h, fixed with 10% formalin, and then stained with 0.1% crystal violet. Images (A-D) (200 × magnification) were acquired with an Olympus IX2-UCB microscope, and invasion capabilities were compared for different treatments (E). Values are mean ± SD of six treatments. *P < 0.05, **P < 0.01, and ***P < 0.001 (one-way ANOVA).

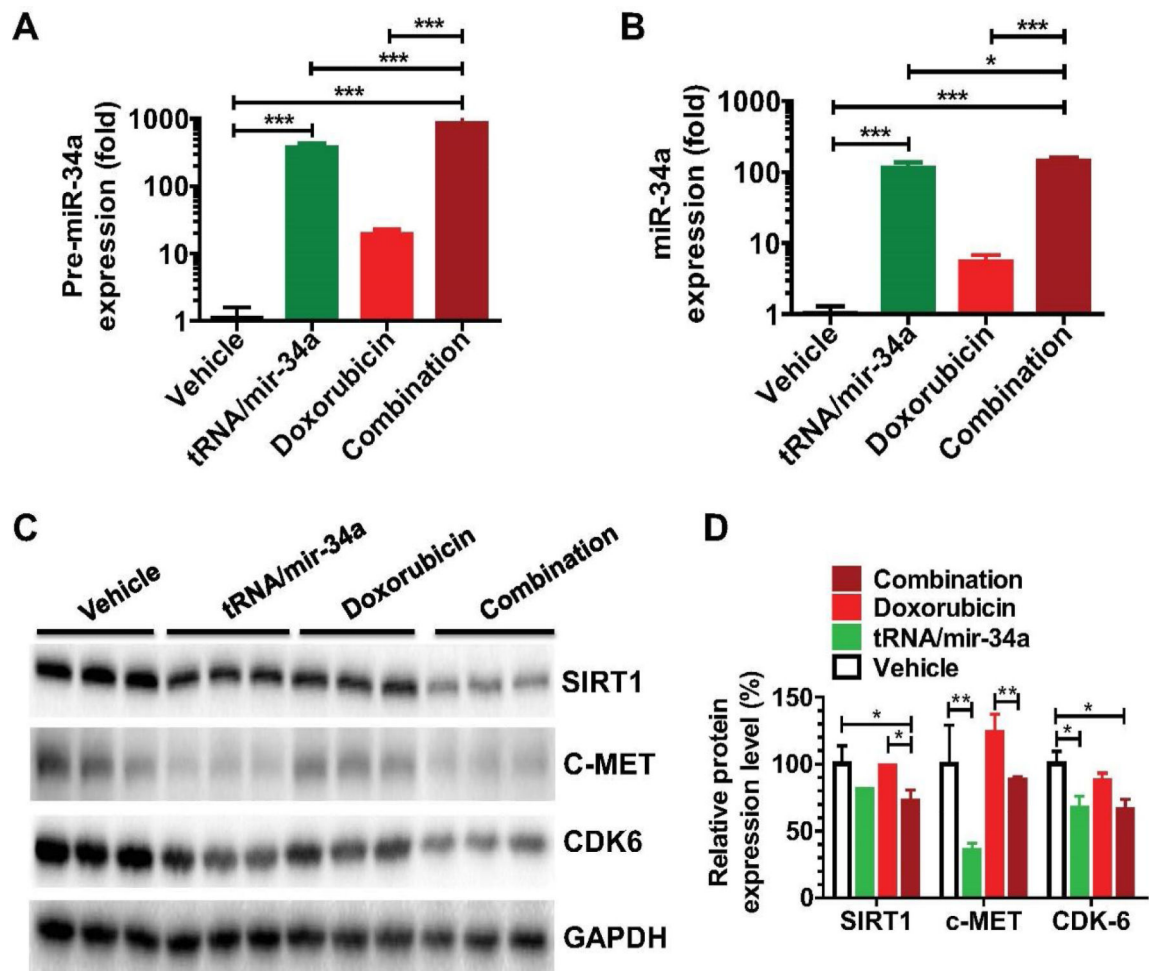


Figure 7.

Comparison of miR-34a and target oncogene expression levels in 143B cells treated with bioengineered miR-34a prodrug (tRNA/mir-34a) and doxorubicin, alone or in combination. Cells were harvested at 72 h after treatment. Pre-miR-34a (A) and mature miR-34a (B) expression levels were quantitated by selective RT-qPCR and stem-loop RT-qPCR assay, respectively. Proteins of miR-34a target genes including SIRT1, c-MET, and CDK6 (C) were measured by Western blot. Band density was determined by Image Lab software (Bio-Rad), and normalized to that of GAPDH (D). Values are mean \pm SD of triplicate treatments. * $P < 0.05$, ** $P < 0.01$, and *** $P < 0.001$ (one-way or two-way ANOVA).

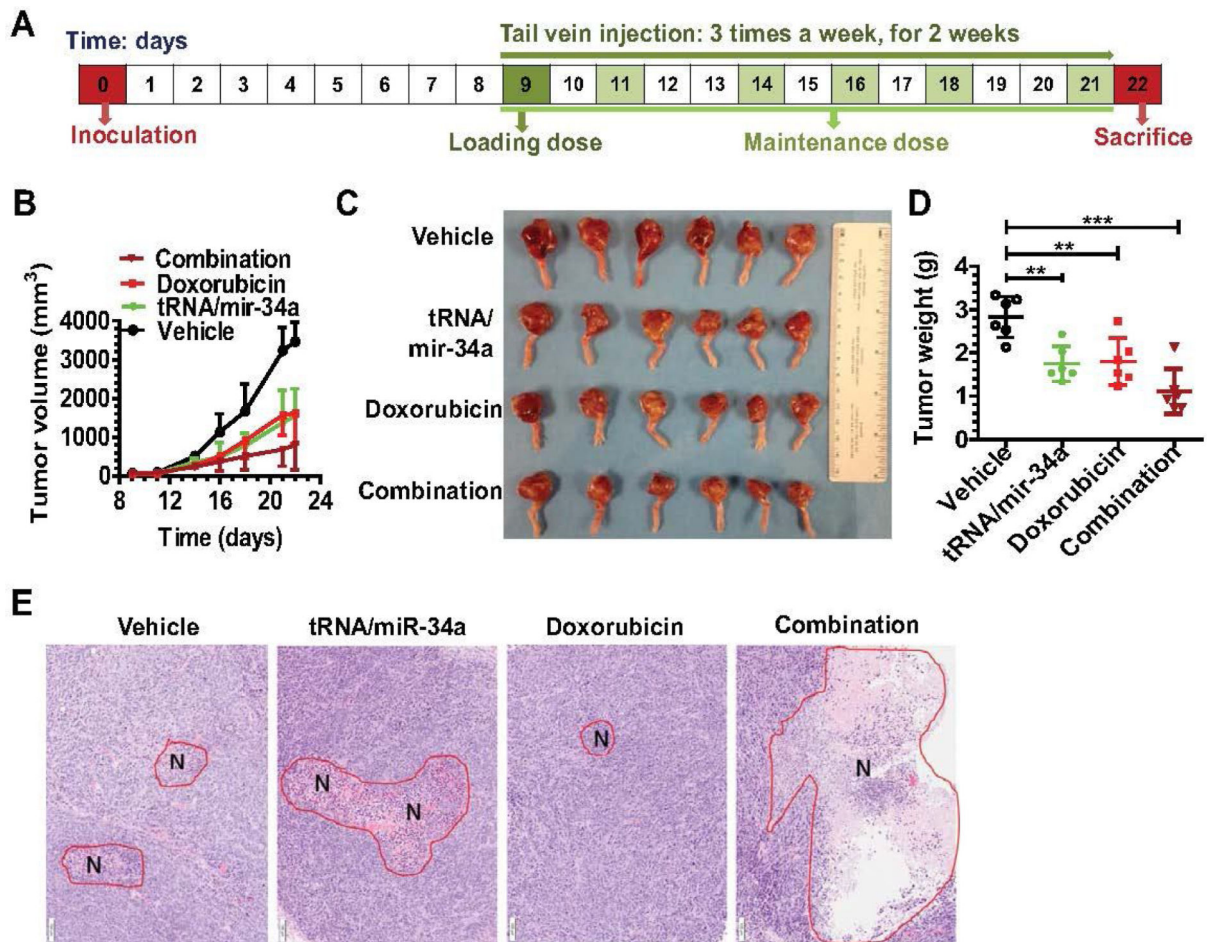


Figure 8. Combination therapy with bioengineered miR-34a prodrug and doxorubicin was more effective to suppress orthotopic osteosarcoma xenograft tumor growth in mice. (A) Timeline of osteosarcoma cell inoculation and drug treatment. (B) Xenograft tumor growth was reduced to a significantly ($P < 0.01$, two-way ANOVA) greater degree by combination therapy than doxorubicin or tRNA/mir-34a alone. (C) Comparison of dissected orthotopic tumor tissues from mice with different treatments. (D) Weights of the dissected xenograft tumors. $**P < 0.01$, and $***P < 0.001$ (one-way ANOVA). (E) H&E histology (100x) showed a much higher degree of tumor necrosis (red circle labeled with N) for xenografts dissected from mice with combination therapy. Values are mean \pm SD ($N = 6$ in each group).

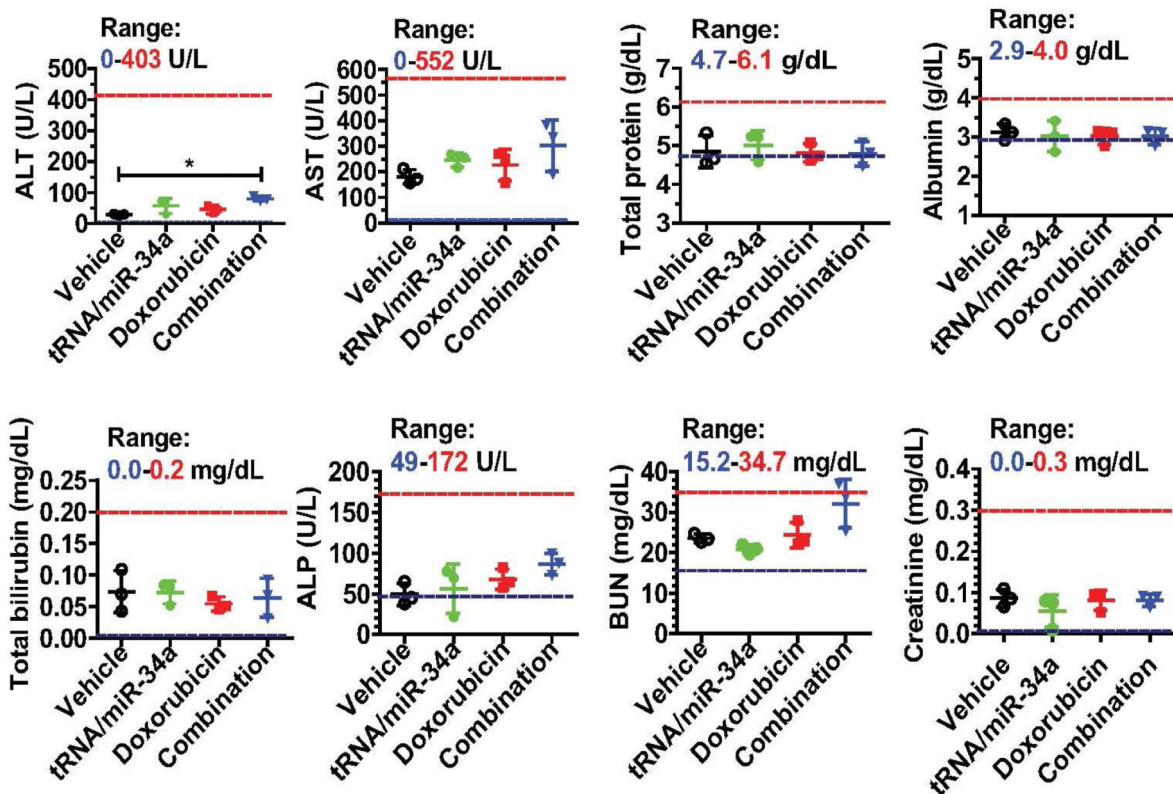


Figure 9. Systemic co-administration of genetically engineered miR-34a prodrug and doxorubicin had no or minor impact on mouse blood chemistry profiles including alanine transaminase (ALT), aspartate transaminase (AST), total protein, albumin, total bilirubin, alkaline phosphatase (ALP), blood urea nitrogen (BUN), and creatinine levels. Values are mean ± SD (N = 3 in each group). *P < 0.05 (one-way ANOVA). The ranges of individual markers (derived from BALB/c mice; Comparative Pathology Laboratory at UC-Davis) were marked as references.